

Evaluation of different approaches for estimating and mapping crop water status in cotton with thermal imaging

V. Alchanatis · Y. Cohen · S. Cohen · M. Moller · M. Sprinstin · M. Meron · J. Tsipris · Y. Saranga · E. Sela

Published online: 3 March 2009
© Springer Science+Business Media, LLC 2009

Abstract Canopy temperature has long been recognized as an indicator of plant water status, therefore, a high-resolution thermal imaging system was used to map crop water status. Potential approaches for estimating crop water status from digital infrared images of the canopy were evaluated. The effect of time of day on leaf temperature measurements was studied: midday was found to be the optimal time for thermal image acquisition. Comparison between theoretical and empirical approaches for estimating leaf water potential showed that empirical temperature baselines were better than those obtained from energy balance equations. Finally, the effects of angle of view and spatial resolution of the thermal images were evaluated: water status was mapped by using angular thermal images. In spite of the different viewing angles and spatial resolution, the map provided a good representation of the measured leaf water potential.

Keywords Cotton · Leaf water potential · Site-specific irrigation · Water stress · CWSI · Infrared thermography · Canopy temperature · Remote sensing

V. Alchanatis (✉) · Y. Cohen · E. Sela
Institute of Agricultural Engineering, ARO, The Volcani Center, P.O. Box 6, Bet Dagan 50250, Israel
e-mail: victor@volcani.agri.gov.il

S. Cohen · M. Moller
Institute of Soil, Water and Environmental Sciences, ARO, The Volcani Center, P.O. Box 6,
Bet Dagan 50250, Israel

M. Sprinstin
The J. Blaustein Institute for Desert Research, Ben-Gurion University of the Negev,
Sede-Boker Campus, 84990 Beersheba, Israel

M. Meron · J. Tsipris
Galilee Technology Center, Migal, P.O. Box 90000, Rosh Pinna 12100, Israel

Y. Saranga · E. Sela
Faculty of Agriculture, The Hebrew University of Jerusalem, Jerusalem, Israel

Introduction

Site-specific irrigation may be defined as a procedure in which irrigation timing and amount are matched to actual crop needs within the smallest feasible management unit, to achieve the desired crop responses. Enhancing productivity in terms of yield and quality per unit of applied water will depend on the ability to map the variability of the crop water status and on the development of site-specific water application technology. Implementation of site-specific irrigation systems could contribute to reduce the water shortage crises in agricultural production.

The spatial variability of crop water status results from variability of soil, crop canopy, topography, irrigation non-uniformity (whether inherent to the application method or due to malfunctions) and other factors such as salinity, which typically is spatially variable. Irrigation-water distribution can be improved by directly monitoring crop water status rather than by measuring soil water content (Jackson 1982). Canopy temperature has long been recognized as an indicator of plant water status (Gates 1964). Following that, a temperature-based crop water stress index was developed (Idso et al. 1981; Jackson et al. 1981). Crop temperature measurements with thermal infrared thermometers (IRTs) are reliable and non-invasive, but they are usually based on a few point measurements and therefore depend on the assumption of uniformity of soil water content and plant density over large areas. In order to map crop water status variability at an adequate resolution, many distributed IRTs are required (Evans et al. 2000). In contrast, remote thermal imagery provides spatial information of surface temperature and thus enables mapping of canopy temperature variability over large areas. However, in order to make these thermal images useful for supporting variable-rate irrigation (VRI) in space and time, identification and assignment of irrigation zones is required. The process of transformation of raw thermal imagery to irrigation zones comprises three main phases, each related to a wide research area: (1) definition of crop water status according to temperature; (2) characterization of the spatial variability pattern of water status in the field; and (3) delineation of irrigation zones. This study focuses on phases 1 and 2.

One of the best known indices for evaluating crop water stress is the Crop Water Stress Index (CWSI), which expresses the difference between “well-watered baseline” and “total stress” temperatures and is normalized against vapor pressure deficit (Idso et al. 1981; Jackson et al. 1981; Jones et al. 2002). As formulated and applied originally, it encountered the following problems. (1) Poor separation of the relevant crop canopy temperatures from those of the general leaf population and the soil background when the measurements were done with hand-held or high-altitude airborne radiometers, which combined them all together into one analysis element, (Clarke 1997). (2) Under changing atmospheric conditions, normalization of CWSI is much more complicated than use of vapor pressure deficit (VPD) alone (Jackson et al. 1988; Jones 1999a).

A new approach presented in recent studies relies on better temperature separation by means of novel imaging equipment, and use of Artificial Wet Reference Surface (AWRS) for calculating the CWSI (Cohen et al. 2005; Meron et al. 2003; Möller et al. 2007). Clawson et al. (1989) suggested the use of natural reference surfaces, such as well-watered crop sections, for CWSI normalization, but they are difficult to maintain. Meron, Tsipris and Fuchs (unpublished report to the Ministry of Science, Israel 1994) used dry and wet artificial reference surfaces (ARSs) with known reflectances and aerodynamic attributes, and reformulated the energy balance equation so as to ascribe to CWSI theoretical

minimum and maximum values of 0 and 1 (Meron et al. 2003). In a similar approach, greased and wetted single-leaf references were used by Jones (1999b). From a practical standpoint, the ARS method seems suitable for large-scale application, as it provides flexible deployment and reproducible surfaces. Recent work has shown that the CWSI approach can be expanded in order to determine a soil water status index (Colaizzi et al. 2003) and the depth of root-zone water depletion; additions that may improve our ability to determine irrigation amounts.

Another approach was based on the relationship between variability in fine-resolution measurements of canopy temperature and crop water stress in cotton fields in central Arizona, USA (Gonzalez-Dugo et al. 2006). By using both measurements and simulation models, these authors compared the standard deviation of the canopy temperature to the more complex and data-intensive CWSI. This approach was found useful only for moderately stressed crops, for which there was a linear relation between canopy-temperature variations and field-scale CWSI. The effects of low and high stress were not addressed in depth.

As new irrigation-scheduling tools, CWSI-derived indices need verification, through comparison with and integration into existing and accepted measures of crop water stress. Leaf and Stem water potentials (LWP if measured on bare leaves, SWP when measured on pre-wrapped leaves), are generally accepted as directly measurable crop stress measures and are quite well calibrated for field crops such as cotton (Grimes and Yamada 1982) and a range of fruit crops (Naor et al. 1995; Stern et al. 1998). Calibration of thermal indices against LWP may be empirical (Cohen et al. 2005) or theoretical, based on energy-balance models (Möller et al. 2007).

Thermal sensing with high-resolution thermal imaging systems had limited practical use in agriculture until recently, because of the technological problems presented by the bulk of cooled IR systems that could provide the required spatial and thermal accuracy. The recent development of uncooled thermal imaging systems based on micro-bolometers reduced the cost of the systems and, more importantly, made them easy to use in field conditions. Their relatively high spatial and thermal resolution enables radiometric measurement of temperatures with typical accuracy of 0.1°C.

Objective

The general objective of this work was to evaluate and compare a number of potential approaches to the estimation of crop water status by using digital infrared or thermal images of the crop canopy. These images, in turn, can be used to create a map of leaf water potential to support irrigation scheduling decisions.

The specific objective of the present study was to characterize the practical issues to be addressed in evaluating crop water status. First, the effect of the time of day on the accuracy of predictions of leaf water potential based on leaf temperature measurements was studied. Second, two approaches were compared: a theoretical approach that involved the application of mathematical tools and energy balance equations to measured meteorological data to estimate leaf water potential; and an empirical approach that used measurements of the temperature of an artificial wet surface and of the ambient air in order to estimate leaf water potential. Finally, the effects of angle of view and spatial resolution of the thermal images were evaluated.

Materials and methods

Field plots

Field measurements were conducted in summer 2003 on a clay loam soil at Kibbutz Shamir, Upper Galilee, Israel (33.163175°N; 35.638490°E), where there is a Mediterranean climate. The measurements were carried out on two dates: July 15 and August 6, 2003.

Plots planted with cotton (*Gossypium barbadense* L. cv. PF-15) were drip irrigated with one lateral between every two rows. Each treatment was 6 m wide (six rows, spaced 1 m apart) by 20 m long. The crop was grown in accordance with normal practices, with daily water application equal to the daytime potential evapo-transpiration. Five water-treatments were applied with two replicates (Table 1). One treatment—designated as Tr-D—served as an unstressed reference and was over-irrigated through two drip laterals per row pair, instead of one. A second treatment, designated as Tr-0, represented the common practice of daily irrigation equal to the potential evapo-transpiration. Towards the day of field measurements, three stressed treatments, designated as Tr-2, Tr-4 and Tr-6, were induced by suppressing irrigation for 2, 4, and 6 days, respectively. After the field measurements, the plots were compensated for water and fertilizer that was ceased, so that all the treatments received the same total amount of water and nitrogen.

The treatments were in contiguous areas containing 10 plots arranged in end-to-end pairs in the row direction, with five such pairs side-by-side perpendicular to the row direction. All plots received the same amount of nitrogen fertilizer through the irrigation system.

Thermal image acquisition

Thermal images of the plots were taken with an uncooled infrared thermal camera (ThermaCAM model PM545, FLIR Systems, Sweden) equipped with a 320 × 240 pixel microbolometer sensor, sensitive in the spectral range of 7.5–13 μm and a lens with an field of view of 24°. The camera was mounted 5 m above the ground, pointing vertically downwards. The canopy height was about 1 m, so that the linear field of view at the canopy level was 5 mm/pixel (field of view of $2 * (5 - 1) * \tan(24^\circ/2) = 1.7$ m). This resolution enabled us to distinguish between leaves and soil and to select pixels that contained only leaves for further analysis.

Leaf samples

Five youngest, fully expanded leaves were selected in each plot and their petiole tagged with a piece of aluminum foil to enable their identification in the thermal image.

Table 1 Irrigation treatments and their symbol in the text

Days with no irrigation	Treatment symbol in text
6	Tr-6
4	Tr-4
2	Tr-2
0	Tr-0
0 (double amount)	Tr-D

Subsequent to the thermal image acquisition, the tagged leaves were cut and their LWP measured with a pressure chamber (model ARIMAD 1, Mevo Hama Instruments, Israel), as described by Meron et al. (1987). The measurements were conducted during the morning (1000–1200 local time, GMT + 2 h) and around the time of solar zenith (1200–1400 local time, GMT + 2 h).

Meteorological conditions and CWSI

Global solar radiation, wind speed, air temperature and relative humidity were measured 2 m above the ground (0.5 m above the canopy) by a meteorological station positioned within the experimental plot. The sampling rate was 0.1 Hz, and 1-min averages were recorded by a data acquisition system (CR10X, Campbell Scientific, Logan, UT, USA).

Processing of thermal image data

The thermal images were processed with digital image-processing tools. The raw thermal image data were obtained in FLIR Systems' proprietary format and converted to gray-scale images in which each gray level interval represented 0.1°C. This conversion was performed by (a) setting the temperature span of the images and saving them as bitmap images (BMP format) by means of ThermaCamExplorer software (FLIR Systems, Sweden), and (b) converting the bitmap images to 8-bit uncompressed TIFF format by means of Adobe Photoshop 7.0 software (Adobe Inc.) The images were then processed with two software packages: (a) Matlab R13 software (The Mathworks Inc., Natick, MA, USA); and (b) IMAGINE 8.7 software (Leica Geosystems AG, Heerbrugg, Switzerland). The temperature of each pixel was first calculated from the 8-bit gray-scale image, by using the following equation:

$$T(x, y) = T_{\min} + \frac{T_{\text{span}}}{255} GL(x, y) \quad (1)$$

where $T(x, y)$ —calculated temperature at pixel (x, y) ; $GL(x, y)$ —gray level of pixel (x, y) in the 8-bit TIFF image; T_{span} —temperature span in the image, as set in the ThermaCamExplorer, which was always set to 25.5°C; T_{\min} —temperature corresponding to gray level 0; 255 the maximum value of gray level in an 8-bit gray-scale image.

LWP regression models

The temperatures of individual leaves in the images were extracted, in order to establish the relationship between measured and estimated LWP. The leaves that were tagged with aluminum foil were manually segmented in the digital IR images and their mean temperatures, along with additional descriptive statistics (variance, minimum, maximum) were calculated. These values were used to calculate the crop water stress index (CWSI) and to formulate regression models for LWP prediction.

The crop water stress index CWSI was calculated according to Jones (1992) as:

$$\text{CWSI} = \frac{T_{\text{canopy}} - T_{\text{wet}}}{T_{\text{dry}} - T_{\text{wet}}} \quad (2)$$

where T_{canopy} is the actual canopy temperature obtained from the thermal image and T_{wet} and T_{dry} are the lower and upper boundary temperatures, corresponding to a fully transpiring leaf with open stomata and a non-transpiring leaf with closed stomata, respectively. Note that T_{wet} and T_{dry} are equivalent to T_{base} and T_{max} in the original formulation of CWSI

by Idso et al. (1981). A wet artificial reference surface (WARS) was constructed as described by Meron et al. (2003), and placed in the camera field of view when thermal images were acquired. A 5 cm thick slab of expanded polystyrene foam was floated in a $40 \times 30 \times 12$ cm plastic tray, covering most of the water surface. It was coated with a doubled piece of 0.5 mm thick water absorbent non woven polyester and viscose mixture cloth (Spuntech, Israel), overlaid on another 2 mm thick polyester non-woven water-absorbent cloth. The edges of the clothes served as a wick, soaking up water to replace evaporation, and the polystyrene foam insulated the float from the background. This floating setup provided horizontal and vertical alignment and a permanently wet surface of reproducible radiometric and physical properties. The fuzzy material “skin layer” measured by IR imaging has no appreciable mass, thus its thermal inertia is negligible. Its average temperature was obtained from the thermal images and was used as T_{wet} in Eq. 2. Ehrler et al. (1978) and Irmak et al. (2000) found that the upper base level ($T_{\text{canopy}} - T_{\text{air}}$) when transpiration has ceased, was relatively constant, in the range of +4.6 to +5.0°C. In the present study, as in Cohen et al. (2005) and Möller et al. (2007), T_{dry} was estimated by adding 5.0°C to the dry bulb temperature of air: $T_{\text{dry}} = T_{\text{air}} + 5^\circ\text{C}$. Alternative estimates for T_{wet} and T_{dry} based on energy balance equations were also tested, following Jones (1999b). Specifically, T_{wet} was derived from the following equation:

$$T_{\text{wet}} = T_a + \frac{r_{\text{HR}} r_{\text{aW}} \gamma R_{\text{ni}}}{\rho_a c_p [\gamma (r_{\text{aW}}) + \Delta r_{\text{HR}}]} - \frac{r_{\text{HR}} \text{VPD}}{\gamma r_{\text{aW}} + \Delta r_{\text{HR}}} \quad (3)$$

where T_a is air temperature, r_{HR} is the resistance to radiative heat transfer (Jones 1992, 1999b), based on a characteristic leaf dimension of 0.1 m, r_{aW} is the boundary layer resistance for water vapor (Jones 1992), γ is the psychrometric constant, R_{ni} is net radiation, ρ_a is the density of air, c_p is the specific heat of air and Δ is the slope of the saturation vapor pressure curve.

T_{dry} was also theoretically estimated on the assumption of isothermal radiation (Jones 1999b):

$$T_{\text{dry}} = T_a + \frac{r_{\text{HR}} R_{\text{ni}}}{\rho_a c_p} \quad (4)$$

A CWSI that uses the measured values of T_{wet} and T_{dry} is referred to as CWSI_ARS and CWSI that uses Eqs. 3 and 4 for determining T_{wet} and T_{dry} is referred to as CWSI_I₂.

Oblique images and LWP mapping

To cover larger areas and to evaluate the effect of spatial resolution and angle of acquisition, diagonal thermal and RGB images were acquired in a cotton field in Kibbutz Revadim, in the northern Negev (31.778020°N; 34.824891°E) on August 15, 2005. The crop was at the boll-filling stage. Three irrigation treatments, each with four replicates, included: 1—well watered (100% of the application required); 2—moderate stress (81% of the required application); and 3—high stress (63% of the required application). An image of the experimental area (60 × 80 m), consisting of 12 experimental plots, was acquired from a crane elevated at a height of 20 m. The camera was inclined at an angle of about 60° from the vertical. A wide-angle lens (45°) was used. This arrangement yielded images with spatial resolution much lower than that obtained in the vertical images: whereas vertical images acquired from 5 m above the canopy had a spatial resolution of about 5 mm per pixel, the spatial resolution of images acquired obliquely from 20 m above the

canopy was about 50 times lower. In addition, the oblique viewing angle resulted in varying spatial resolution across the image, ranging between 0.20 and 0.40 mm per pixel for areas close to or remote from the camera, respectively.

CWSI was calculated for each pixel by using Eq. 2. The low spatial resolution did not enable the use of the ARS as the wet reference, therefore, as suggested by Clawson et al. (1989) the average canopy temperature of the lowest decile was used as the wet reference. The dry temperature was approximated by $T_{\text{air}} + 5^{\circ}\text{C}$. Then, the LWP of each pixel was calculated by using the regression model that links CWSI and LWP, which was constructed from the midday data acquired in 2003.

Water status maps were obtained by assigning each pixel to one of five pre-determined categories according to LWP:

- LWP > -1.4 MPa represents over-irrigated plants (Oir);
- 1.4 MPa \geq LWP > -1.7 MPa well watered plants (WW);
- 1.7 MPa \geq LWP > -2.0 MPa low water stress (LWS);
- 2.0 MPa \geq LWP > -2.3 MPa medium water stress (MWS);
- 2.3 MPa \geq LWP severe water stress (SWS).

The LWPs of eight experimental plots were evaluated from the map: the central part of each sub-plot was extracted from the image (inner polygons in the image, Fig. 7) and the average value of LWP was calculated. The calculated LWP values generated from the map were compared with actual LWP measurements taken at the same time.

Results and discussion

Distribution of measured leaf water potential in irrigation treatments

The various irrigation treatments created a wide range of water statuses as reflected by leaf water potential and CWSI values calculated from leaf temperature (Table 2). LWP reflected similar trends in both measuring days. Duncan's multiple range test divided the five treatments into three distinct groups. Leaves from Tr-2 and Tr-0 presented similar LWP values, which suggests that after 2 days with no irrigation, cotton leaves did not show

Table 2 Values of leaf water potential (LWP) and crop water stress index (CWSI) measure in 2 days in cotton under various irrigation treatments. Means ($n = 5$) accompanied by different letters (a, b, c) are significantly different ($p < 0.05$) according to Duncan's multiple range tests

	Irrig. treat.	LWP Avg.	CWSI Avg.
July 15 2003	Tr-6	-2.26 a	0.52 a
	Tr-4	-2.20 a	0.43 a
	Tr-2	-1.59 b	0.20 b
	Tr-0	-1.62 bc	0.10 b
	Tr-D	-1.40 c	0.10 b
August 6 2003	Tr-6	-2.29 a	0.58 a
	Tr-4	-2.08 a	0.50 a
	Tr-2	-1.34 b	0.12 b
	Tr-0	-1.33 b	0.18 b
	Tr-D	-0.83 c	-0.23 c

stress. However, after 4 or 6 days with no irrigation (Tr-4 and Tr-6, respectively) the plants showed progressive stress. This transition reflects the vital necessity of water status monitoring to enable precise irrigation scheduling and thereby to prevent damage. Leaves from Tr-D showed considerably higher LWP as compared with Tr-0 (significant in the second day), which indicates the effect of irrigation amounts on water status.

Effect of time of day

The first objective of this work was to evaluate the thermal indices that were derived from thermal imaging, in order to estimate water status during two different points in time: morning and midday. Figure 1a shows the linear regression statistical models that were built for two different dates, in order to estimate LWP from temperatures measured in the morning (10:00–12:00). By referring to each date individually, one can observe that the regression model for August has a better fit to the data than that for July. Also, the models obtained for each of the days differed in terms of slope and intercept. This means that the relationship between the thermal index CWSI and water status as expressed by morning LWP differed between the two dates. Figure 1b shows the linear regression statistical models for midday (12:00–14:00). The models for the two days are very similar: they have the same slope and differ only slightly in their intercepts—a difference of 0.1 Mpa. This result shows that the relationship between midday LWP and CWSI was stable across the two measuring days.

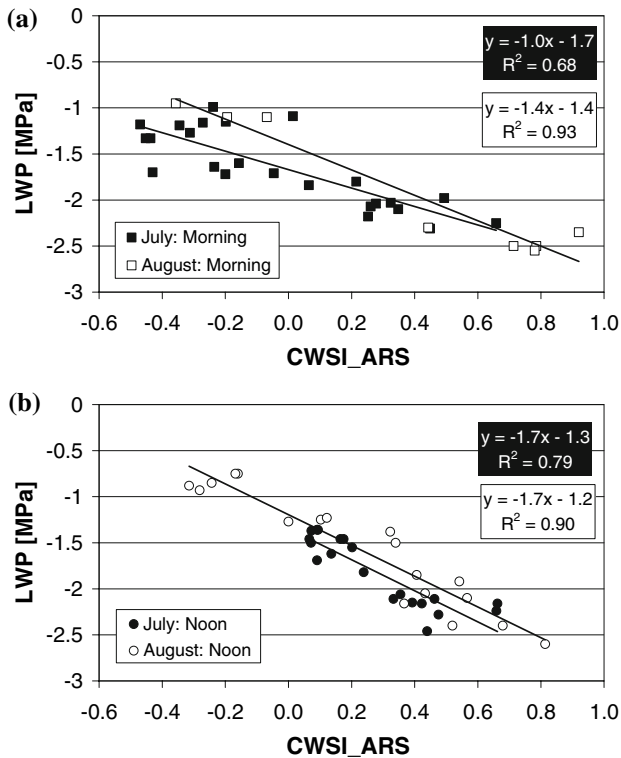


Fig. 1 Linear regression statistical model of CWSI for evaluating leaf water potential: **a** morning and **b** around midday

The two models (morning and midday) can also be compared with respect to their standard errors. When data from the two dates (July and August) are combined to form a single model, the standard error of the morning model is 0.25 MPa whereas that of the midday model is 0.20 MPa. These results show that the midday measurements for estimating water status are significantly more reliable than morning estimates ($p < 0.05$).

Plant water status is normally evaluated at the time of maximum expression of stress (lowest LWP values). In cotton, mid-day LWP is an acceptable measure of plant water status. According to previous findings (Cornish et al. 1991), in the course of the day, the stress in the plants builds up during morning time, to a ~2-h plateau around the solar zenith and then diminishes. The decline in LWP during morning hours is influenced by the climatic conditions which may vary greatly from day to day. In the current study, the observed need for different models may have arisen because of differences between the 2 days in the rates of water stress development in the morning hours. In July, in contrast to August, water stress was not yet fully developed in the morning.

On the other hand, the midday models were stable within the time scale of the present study, that is, virtually the same model applied to both dates. Although this observation was based upon two dates only, it fits the general knowledge and commercial practice where plant water stress is measured during its midday plateau (Girona et al. 2005).

Alternative temperature baselines for CWSI calculation

The CWSI values showed similar separation capabilities to the results of the LWP measurements (Table 2). This indicates the effectiveness of the CWSI to be used as a substitute for direct LWP measurements.

In this paper, we present four different formulations of CWSI; they all require measurement of the canopy temperature but differ in the way the lower and upper baselines— T_{wet} and T_{dry} , respectively—were estimated. Table 3 summarizes the four thermal indices and the way that each reference temperature is calculated. Three of them were approximated from direct measurements of the baselines (i.e., empirical approaches), and one used model-based calculation of the baselines (i.e., a theoretical approach). Empirical formulations are based on direct measurements of the lower baseline temperature (T_{wet}) and estimation of the upper baseline according to air temperature. The theoretical formulation

Table 3 Summary of thermal indices and calculation method of each baseline temperature

Baseline approximation approach		T_{wet}	T_{dry}
Direct measurements	CWSI_ARS	Measured from artificial wet reference adjacent to crop in the image	Air temperature plus five degrees
	CWSI_IRT	Measured from artificial wet reference at fixed point in the field	Air temperature plus five degrees
	CWSI_WW (Clawson)–LWP map	Measured from well watered reference crop	Air temperature plus five degrees
Theoretical calculation	CWSI_I ₂	Calculated from energy balance model (Eq. 2)	Calculated from energy balance model (Eq. 3)

of the index is based on meteorological measurements only and computation of upper and lower baselines according to energy balance equations.

Figure 2 shows the regression model obtained when CWSI_ARS was used and Fig. 3 shows that obtained when CWSI_I₂ was used. The data shown were obtained on both dates at midday. The correlation coefficient of the regression model that used the empirical index CWSI_ARS is better than the one that used the theoretically calculated baselines: r^2 of 0.85 and 0.69, respectively. This superiority is also reflected in the standard errors of the two models: 0.20 and 0.29 MPa, respectively. The coefficients of the regression lines are also different. This means that, in addition to the higher scatter in the values obtained by using the theoretical index, the model characteristics also differed. The slope of the theoretical model was steeper and therefore its sensitivity to CWSI changes was higher, that is, small variations in the values of CWSI lead to large variations in the predicted/estimated LWP.

Jones (1992) argued that CWSI is better related to crop transpiration than to directly estimated water status and is really a measure of $1 - E/E_p$, where E_p is the potential transpiration of the well watered crop. In order to evaluate the correlation of the estimate $1 - E/E_p$ to the two formulations of the thermal index (empirical and theoretical), the two are plotted against $1 - E/E_p$ (Fig. 4—note that the Y-axes for the two indices are shifted vertically in order to separate the two plots). The empirical formulation (CWSI_ARS) is seen to be better correlated to the water status estimate $1 - E/E_p$, which supports the opinion that T_{wet} and T_{dry} are best evaluated from direct measurements of the ARS and air temperature.

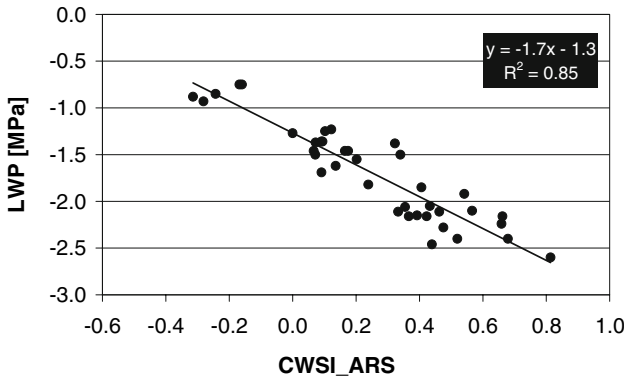


Fig. 2 CWSI calculated using T_{wet} measured with mobile white WARS from the image

Fig. 3 Theoretically formulated stress index I₂, using T_{wet} and T_{dry} calculated from Penman–Monteith model

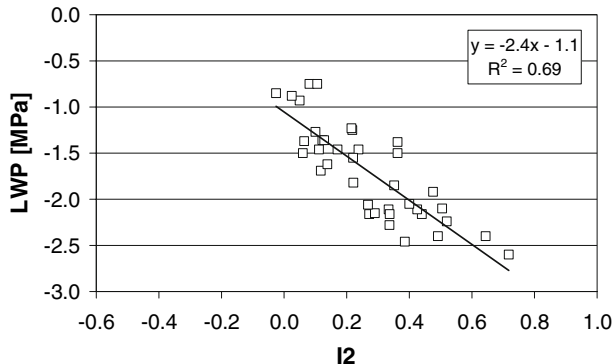
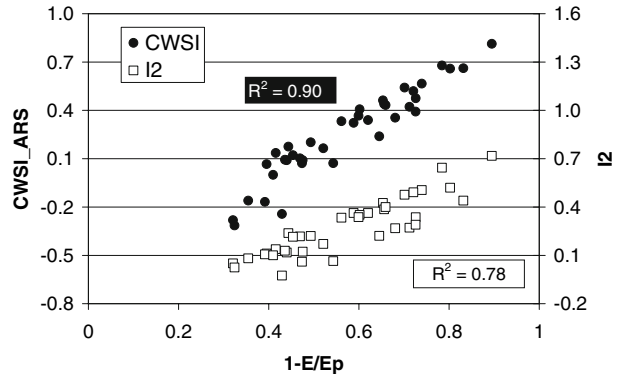


Fig. 4 CWSI with mobile WARS and I_2 versus $1 - E/E_p$



Practical use of the CWSI as a thermal index for estimation of LWP depends on the applicability of the method. The advantage of the empirical approach is that there is no need to monitor local environmental conditions with high temporal resolution. Only air temperature has to be monitored, which does not have wide fluctuations, either temporal or spatial, that is, it is sufficient to measure air temperature once at every given time interval, at just one point in the field. Another advantage is that the measured lower baseline, T_{wet} , incorporates the effects of meteorological factors, such as humidity, wind speed, and radiation. If the reference T_{wet} is measured locally, that is, within the image of the canopy, then it incorporates all the local conditions and best represents the lower baseline.

The advantage of the theoretical approach is that there is no need to simulate a freely transpiring leaf nor to maintain a well-watered plot: the lower and higher baselines are calculated by means of energy balance equations. The practical disadvantage of such an approach is that a sophisticated meteorological station is needed for each field; the closer the station to the point of measurement, the more accurate the input to the energy balance model. In addition to that, the energy balance model of the leaf is based on the assumption that it is in equilibrium with the surroundings: an assumption that is not always true. Also, some typical parameters of the leaves, such as heat transfer resistance and aerodynamic coefficients, are empirically estimated and their robustness may be limited. Energy balance models are based on the assumption of a typical leaf which, in practice, is a virtual leaf that represents an average. Deviation from the assumed leaf parameters might also lead to inaccuracies. Nonetheless, if the derived indices can be used for reliable determination of water status, then the specific requirements for implementing such an approach have to be considered.

From a practical standpoint, the need to have an ARS always available in the image may be a limiting factor in terms of the applicability of the method. An alternative would be to keep a stationary ARS in the field and to measure its temperature with an infrared thermometer (IRT). Figure 5 shows the regression model of the LWP against the thermal index with a stationary T_{wet} (CWSI_IRT). The correlation coefficient is lower than that of the regression obtained with the mobile ARS (r^2 of 0.68 and 0.85, respectively). Thus, the use of a stationary ARS placed in the field for estimating T_{wet} seems to be less accurate than using the mobile ARS in the image.

If the reference T_{wet} is measured in the vicinity of the crop but not adjacent to the canopy when the temperature of the latter is measured, then the instantaneous local conditions may not be identical to those adjacent to the canopy and, therefore, may bias the results. Nevertheless, this T_{wet} value is not affected by assumptions of the energy balance

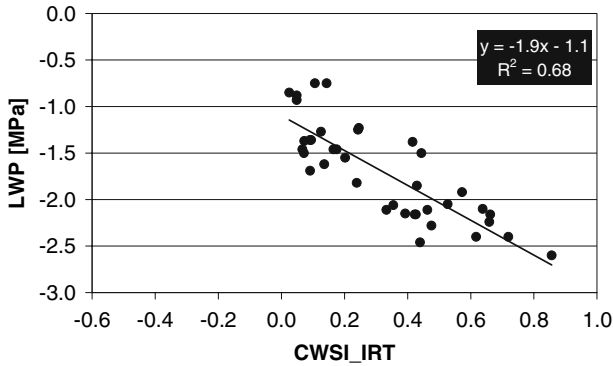


Fig. 5 CWSI_IRT calculated using T_{wet} measured with static WARS

equations, such as being in an equilibrium state, or by the heat transfer resistance values of the various boundary layers.

The effect of spatial resolution and angle of view

Figure 6 shows a water status map (expressed in terms of LWP), superimposed onto a color digital image acquired from the same location. The map was created from a thermal image of irrigation plots acquired from an oblique viewpoint. Visual observation of Fig. 6 shows that the various irrigation treatments can be readily recognized on the map and that, in general, each treatment is associated with an appropriate LWP class.

Figure 7a compares the water status as calculated from the remote TIR image with the measured values of LWP in eight sub-plots. Ground measurements of LWP showed that

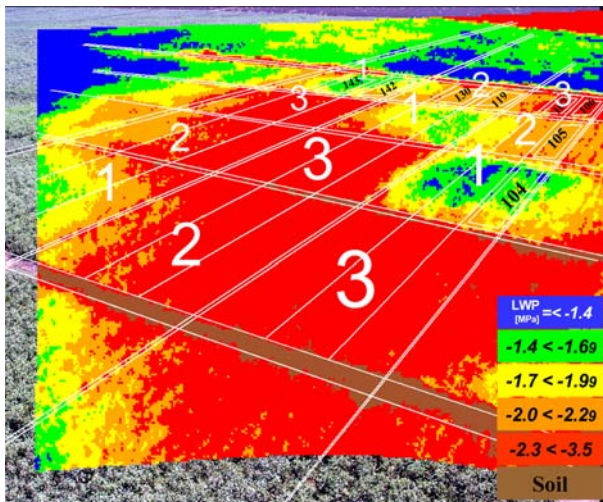


Fig. 6 LWP map of experimental plots in Revadim on August 15, 2005. Digits indicate irrigation treatment: 1—well watered (100% of the required amount), 2—moderate stress (81% of the required amount) and 3—high stress (63% of the required amount). Grid lines indicate borders of irrigation treatments, and inner squares indicate areas that were sampled for calculation of average LWP values

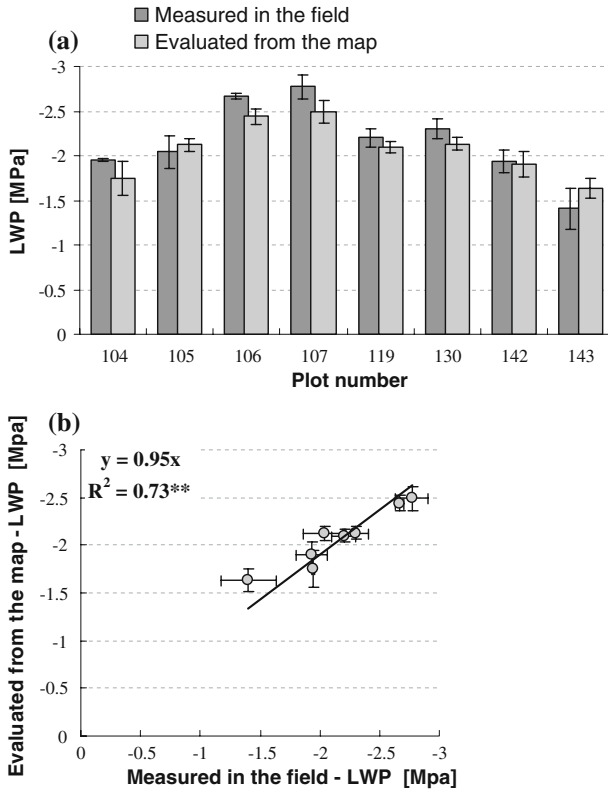


Fig. 7 Comparison between map-based LWP evaluation and ground measurements for three irrigation treatments, on August 15, 2005. Vertical bars represent standard deviation values

the average values ranged from -1.4 MPa (plot 143) to -2.7 MPa (plot 107). The difference in measured water status between the irrigation treatments was statistically significant ($p = 0.05$). Figure 7b compares measured and predicted values of LWP. The vertical error bars represent the variability of the LWP as calculated from the pixels of the sub-plot; the horizontal bars represent the variability of the LWP measurements in the field (based on four leaves per sub-plot). When the intercept value is forced to zero, the coefficient of the regression equation (slope) becomes statistically significant ($p < 0.01$). The value of the slope is 0.95, which indicates that the model slightly underestimates the water status, that is, the predicted values are slightly lower than those measured in the field. The coefficient of determination (r^2) is 0.73, which indicates that the predicted values are slightly dispersed around the 1:1 diagonal.

With regard to the water status groups, six out of eight pairs belong to the same group. As for the two remaining pairs (plots 130 and 143, although the measured and evaluated values fell into the same water status group) the measured values were equal to those of the upper and lower group border, respectively.

The conditions under which the map was made are different from those for which the LWP model was developed. (1) Different geo-climatic sub-regions: the model was developed in a high, mountain area whereas the map represents a coastal plain area. More specifically, there were differences between the experimental studies in wind speed and

VPD range. (2) Different image acquisition modes: the model was based on images acquired by a vertically oriented camera, whereas the image for the map was acquired with an obliquely oriented camera. The differences in viewing angle affect the spatial resolution. The model was based on a very high resolution that enabled single leaves to be readily detected, whereas the map was based on a coarser resolution, so that each pixel could be either a mixture of several leaves under varied illumination or a mixture of canopy and bare soil. (3) Different CWSI calculations (Table 3): whereas the model was developed with a WARS, the map was based on the lowest temperature decile as wet reference. When these differences are taken into account, the reported accuracy of LWP mapping can be considered to validate the CWSI-LWP model based on thermal imaging.

Conclusions

This paper summarizes the practical aspects of estimating and mapping water status variability in cotton by means of thermal imaging.

- The period around midday was found to be the optimal time for thermal image acquisition. Although this interval limits the time available for evaluating the water status, it seems that measurement around midday yields better results than morning measurements.
- For model development T_{wet} , as measured with the aid of the mobile WARS, was found to give the best representation of the lower baseline. Use of air temperature plus 5°C as the upper baseline was better than the theoretical estimate.
- A model that was developed based on vertically acquired high-resolution images can be applied to lower-resolution, obliquely acquired images to produce a reliable LWP map of a wide area. However, when using low-resolution images for LWP mapping, CWSI_WW should be calculated (Table 3), that is, T_{wet} is estimated from the well-watered fraction of the canopy in the image.

In order to explore the robustness of the developed models, larger scale measurements must be conducted, in different geographical locations and under different meteorological conditions. Furthermore, the validity of the model for different cotton varieties remains to be tested.

Acknowledgments This research was supported by Research Grant no. TB-8006-04 from BARD, the United States—Israel Bi-national Agricultural Research and Development Fund, and Grant 458-0361-04 from the Chief Scientist of the Israel Ministry of Agriculture and Rural Development. Also, we would like to thank Mr. R. Brikman and Dr. A. Bosak for their help in conducting the field measurements and image acquisition. This paper is contribution no 70408 from the ARO, Volcani Center, Bet Dagan 50250, Israel.

References

- Clarke, T. R. (1997). An empirical approach for detecting crop water stress using multispectral airborne sensors. *Horttechnology*, 7, 9–16.
- Clawson, K. L., Jackson, R. D., & Pinter, P. J. (1989). Evaluating plant water stress with canopy temperature differences. *Agronomy Journal*, 81, 858–863.
- Cohen, Y., Alchanatis, V., Meron, M., Saranga, S., & Tsipris, J. (2005). Estimation of leaf water potential by thermal imagery and spatial analysis. *Journal of Experimental Botany*, 56, 1843–1852. doi:10.1093/jxb/eri174.
- Colaizzi, P. D., Barnes, E. M., Clarke, T. R., Choi, C. Y., & Waller, P. M. (2003). Estimating soil moisture under low-frequency surface irrigation using the CWSI. *Journal of Irrigation and Drainage Engineering*, 129, 27–35. doi:10.1061/(ASCE)0733-9437(2003)129:1(27).

- Cornish, K., Radin, J. W., Turcotte, E. L., Lu, Z., & Zeiger, E. (1991). Enhanced photosynthesis and stomatal conductance of pima cotton (*Gossypium barbadense* L.) bred for increased yield. *Plant Physiology*, 97, 484–489. doi:[10.1104/pp.97.2.484](https://doi.org/10.1104/pp.97.2.484).
- Ehrler, W. L., Idso, S. B., Jackson, R. D., & Reginato, R. J. (1978). Wheat canopy temperature relation to plant water potential. *Agronomy Journal*, 70, 251–256.
- Evans, D. E., Sadler, E. J., Camp, C. R., Millen, J. A. (2000). Spatial canopy temperature measurements using central pivot mounted IRTs. In P. C. Robert, R. M. Rust, & W. E. Larsen (Eds.), *Proceedings of the 5th international conference on precision agriculture*. ASA, CSSA, SSSA, Madison, WI, CDROM. Accessed February 15, 2009, from <http://www.ars.usda.gov/SP2UserFiles/Place/66570000/Manuscripts/2000/Man580.pdf>.
- Gates, D. M. (1964). Leaf temperature and transpiration. *Agronomy Journal*, 56, 273–277.
- Girona, J., Mata, M., del Campo, J., Arbonés, A., Bartra, E., & Marsall, J. (2005). The use of midday leaf water potential for scheduling deficit irrigation in vineyards. *Irrigation Science*, 24, 115–127. doi:[10.1007/s00271-005-0015-7](https://doi.org/10.1007/s00271-005-0015-7).
- Gonzalez-Dugo, M. P., Moran, M. S., Mateos, L., & Bryant, R. (2006). Canopy temperature variability as an indicator of crop water stress severity. *Irrigation Science*, 24, 233–240. doi:[10.1007/s00271-005-0022-8](https://doi.org/10.1007/s00271-005-0022-8).
- Grimes, D. W., & Yamada, H. (1982). Relation of cotton growth and yield to minimum leaf water potential. *Crop Science*, 22, 134–139.
- Idso, S. B., Jackson, R. D., Pinter, P. J., Jr., Reginato, R. J., & Hatfield, J. L. (1981). Normalizing the stress-degree-day parameter for environmental variability. *Agricultural Meteorology*, 24, 45–55. doi:[10.1016/0002-1571\(81\)90032-7](https://doi.org/10.1016/0002-1571(81)90032-7).
- Irmak, S., Haman, D. Z., & Bastug, R. (2000). Determination of crop water stress index for irrigation timing and yield estimation of corn. *Agronomy Journal*, 92, 1221–1227.
- Jackson, R. D. (1982). Canopy temperature and crop water stress. In D. I. Hillel (Ed.), *Advances in irrigation* (Vol. 1, pp. 43–85). New York: Academic Press.
- Jackson, R. D., Idso, S. B., Reginato, R. J., & Pinter, P. J. (1981). Canopy temperature as a crop water stress indicator. *Water Resources Research*, 17, 1133–1138. doi:[10.1029/WR017i004p01133](https://doi.org/10.1029/WR017i004p01133).
- Jackson, R. D., Kustas, W. P., & Choudhury, B. J. (1988). A reexamination of the crop water stress index. *Irrigation Science*, 9, 309–317. doi:[10.1007/BF00296705](https://doi.org/10.1007/BF00296705).
- Jones, H. G. (1992). *Plants and microclimate* (2nd ed., pp. 231–236). Cambridge, UK: Cambridge University Press.
- Jones, H. G. (1999a). Use of thermography for quantitative studies of spatial and temporal variation of stomatal conductance over leaf surfaces. *Plant, Cell and Environment*, 22, 1043–1055. doi:[10.1046/j.1365-3040.1999.00468.x](https://doi.org/10.1046/j.1365-3040.1999.00468.x).
- Jones, H. G. (1999b). Use of infrared thermometry for estimation of stomatal conductance as possible aid to irrigation scheduling. *Agricultural and Forest Meteorology*, 95, 139–149. doi:[10.1016/S0168-1923\(99\)00030-1](https://doi.org/10.1016/S0168-1923(99)00030-1).
- Jones, H. G., Stoll, M., Santos, T., de Saousa, C., Chaves, M. M., & Grant, O. (2002). Use of infrared thermography for monitoring stomatal closure in the field: Application to grapevine. *Journal of Experimental Botany*, 53, 2249–2260. doi:[10.1093/jxb/erf083](https://doi.org/10.1093/jxb/erf083).
- Meron, M., Grimes, D. W., Phene, C. J., & Davis, K. R. (1987). Pressure chamber procedures for leaf water potential measurements of cotton. *Irrigation Science*, 8, 215–222. doi:[10.1007/BF00259382](https://doi.org/10.1007/BF00259382).
- Meron, M., Tsipris, J., & Charitt, D. (2003). Remote mapping of crop water status to assess spatial variability of crop stress. In J. V. Stafford & A. Werner (Eds.), *Precision agriculture '03: Proceedings of the 4th European conference on precision agriculture* (pp. 405–410). Wageningen, The Netherlands: Wageningen Academic Publishers.
- Möller, M., Alchanatis, V., Cohen, Y., Meron, M., Tsipris, J., Naor, A., et al. (2007). Use of thermal and visible imagery for estimating crop water status of irrigated grapevine. *Journal of Experimental Botany*, 58, 827–838. doi:[10.1093/jxb/erl115](https://doi.org/10.1093/jxb/erl115).
- Naor, A., Klein, I., & Doron, V. (1995). Stem water potential and apple fruit size. *Journal of the American Society for Horticultural Science*, 120, 577–582.
- Stern, R., Meron, M., Naor, A., Gazit, S., Bravdo, B., & Wallach, R. (1998). Effect of autumnal irrigation level in 'Mauritius' lychee on soil and plant water status and following year flowering intensity and yield. *Journal of the American Society for Horticultural Science*, 123, 150–155.